PROTOTYPE NIR/SWIR LARGE FORMAT ARRAY DETECTOR DEVELOPMENT

Summary Report

Latest update by	A. LAMOURE
Modification date	15/11/2023
Version	2.0
Document Owner	A. LAMOURE
Reference	REC-PRJ-1736
Disclosure & Ownership	This document and any related information are LYNRED property (subject to the rights of any third parties). Its distribution is not a transfer of property. This document can be transmitted to anyone with the need to know. It can be read, disseminated, translated or copied on any media, in whole or in part, provided its owner and integrity be kept. LYNRED shall not be liable for any consequence resulting from the use or inability to use information contained herein.

TABLE OF CONTENT

1 Introduction 3
2 Acronyms 3
3 Reminder Of Detector Design And Manufacturing 4
3.1 Reminder of Detector Design 4
3.1.1 Detection Layer Design 4
3.1.2 ROIC Design 4
3.1.3 Hybridized Prototype Detector design 6
3.2 Reminder of Detector Manufacturing 6
3.2.1 Detection Layer Manufacturing 6
3.2.2 ROIC and Retina Manufacturing 7
3.2.3 Prototype Detector Manufacturing 7
4 Reminder Of Test Means Design And Validation 8
4.1 Reminder of Test Means Design 8
4.2 Reminder of Test Means Validation 12
5 Detector Performance Analysis & Possible Improvements 19
5.1 Reminder of Detector Performances 19
5.1.1 ROIC Performances 19
5.1.2 Detector Performances 20
5.2 Comparison with Planned Performances and Analysis 24
5.3 Consideration of detectors and technologies suitable for science applications 25
5.4 Proposal of possible improvements in performances 25
5.5 Maturity level and applicability to flight model manufacturing 26

1 INTRODUCTION

The purpose of this document is to give a summary report of the development made in the frame of Large Focal Array contract (ALFA project) led by ESA and involving LYNRED, CEA-LETI and CEA-IRFU. As a reminder, the main objectives of this activity were as follows:

- to design and manufacture MCT array detectors to answer the requirements specified in **Erreur ! Source du renvoi introuvable.**.
- to design and manufacture support equipment to operate, test and characterize the manufactured detectors.
- to test and characterize the manufactured detectors to an agreed test plan with reference to the requirements specified in **Erreur ! Source du renvoi introuvable.**.

After a summary of the elements of design, manufacturing, test means development and a synthesis of the detectors test results obtained, an analysis of these results is performed and also a comparison with the planned performances. This analysis allows highlighting the main achievements reached through this study, as well as the possible improvements which could be brought in order to improve the detectors performances.

2 ACRONYMS

CDS	Correlated Double Sampling
CHC	Charge Handling Capacity
CEA	Commissariat à l'Energie Atomique et aux Energies Alternatives
CMP	Chemical Mechanical Process
CTIA	Capacitance Trans-Impedance Amplifier
CZT	Substrate Cadmium Zinc Telluride (CdZnTe)
DAp	Département d'Astro-physique du CEA
DSNU	Dark Signal Non Uniformity
EChO	Exoplanet Characterization Observatory
FEE	Front End Electronics
GR	Generation-Recombination
IR	InfraRed
ITR	Integrate Then Read
IWR	Integrate While Reading
LETI	Laboratoire d'Electronique et de Technologies de l'Information
LFSA	Large Format Sensor Array
MCT	Mercury Cadmium Telluride (HgCdTe)
MIM	Metal-Insulator-Metal
MOS	Metal Oxide Semiconductor
MTF	Modulation Transfer Function
N/A	Not Applicable
PRNU	Photo-Response Non Uniformity
PSF	Point Spread Function

QE	Quantum Efficiency
ROIC	Read-Out Integrated Circuit
RTS	Random Telegraph Signal
SFD	Source Follower per Detector
SOW	Statement Of Work
SWIR	Short Wave InfraRed
TAP	Test Automatique sous Pointe (Probe Test)

3 REMINDER OF DETECTOR DESIGN AND MANUFACTURING

3.1 REMINDER OF DETECTOR DESIGN

3.1.1 Detection Layer Design

The idea of ALFA was to reproduce on a larger scale the best performances of previous programmes. Therefore, diode design is identical to that of TTN4 of NIR LFSA2. The diodes are of the p-on-n type. The only difference with TTN4 is the size of the array that has two implications. The substrate size is larger and the flatness requirements much more stringent, to comply with the hybridization process. The figures of merit taken into account for the design were (1) the dark current itself (2) the QE (3) the PRNU, DSNU, array uniformity the pixel-to-pixel cross-talk, and persistence.

CCN4 detectors are comprised of the following parts (Figure 1) : the MCT absorber material, the ROIC and a solid Ge substrate material to mechanically hold these two elements. The contact pads of the MCT FPA are connected to the Si ROIC via indium bumps. The Si ROIC is thinned out to avoid breakdown during liquid nitrogen cycling. The whole detector is illuminated via the MCT backside surface, which is antireflection coated.

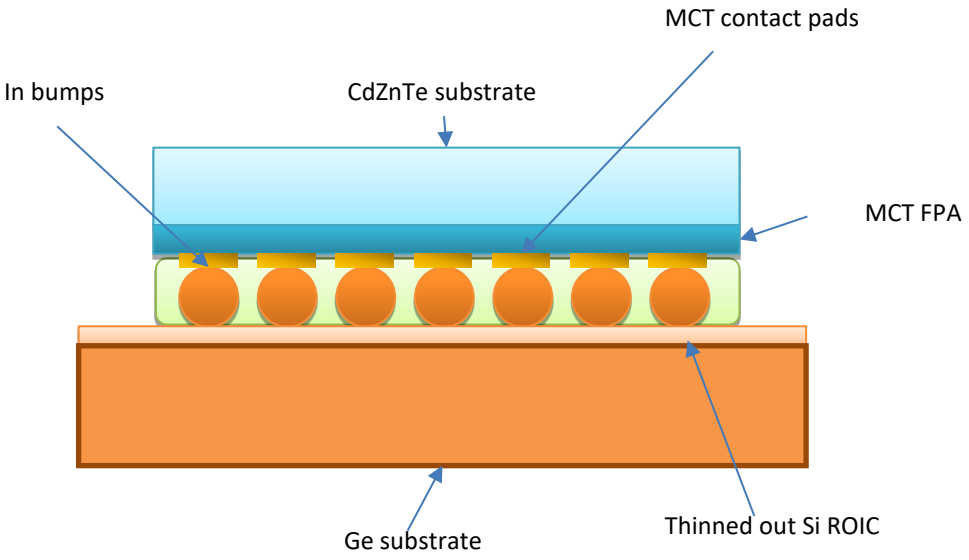

Figure 1 Cross section of a HgCdTe device, with a schematic representation of the MCT contact pads, the In bumps that connect them to the ROIC contacts pads

3.1.2 ROIC Design

The ROIC has been designed for nominal operating at 100K. It has a pixel pitch equal to 15µm and it is compatible with p/n MCT technology diodes which are constituting the Detection Circuit.

A matrix of 2040x2040 sensitive pixels is implemented, where the PV diodes are connected to a Source Follower (SF) transistor by indium bumps. In periphery, reference pixels and test pixels are implemented for ROIC calibration.

The Pixel Array is read row by row with the vertical registers. For each row, the horizontal registers select each column in order to read each pixel.

The reset, integration and reading phases have to be generated by external sequencer according to the selected mode programmed by the digital part.

The available modes are:

- Science Mode: this one is the default mode. It guarantees a low readout noise when operating to 100 KHz. Moreover, the glow generated should be weak because the power consumption is low.
- Fast Mode: operating up to 6MHz. A sample & hold chain is added in each column connected to Video Amplifier.
- Windowing Mode: up to 3 windows can be defined by user.
- Tracking Mode: readout is interlacing full field rows and the windows. At the end of each row, the windows are read.

The data are available with 1, or 4 or 32 outputs.

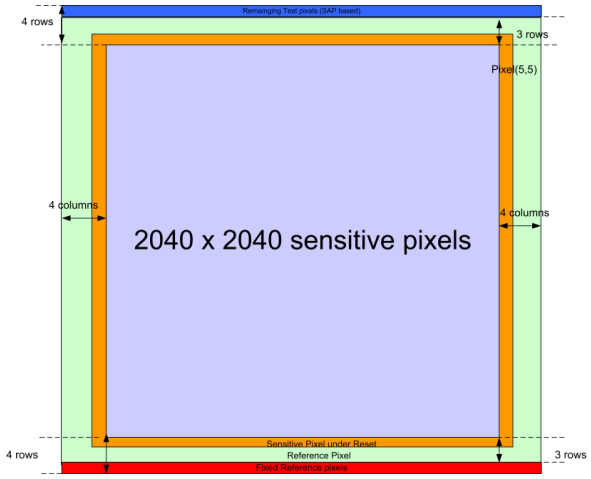

Figure 2: ROIC Matrix Array Architecture

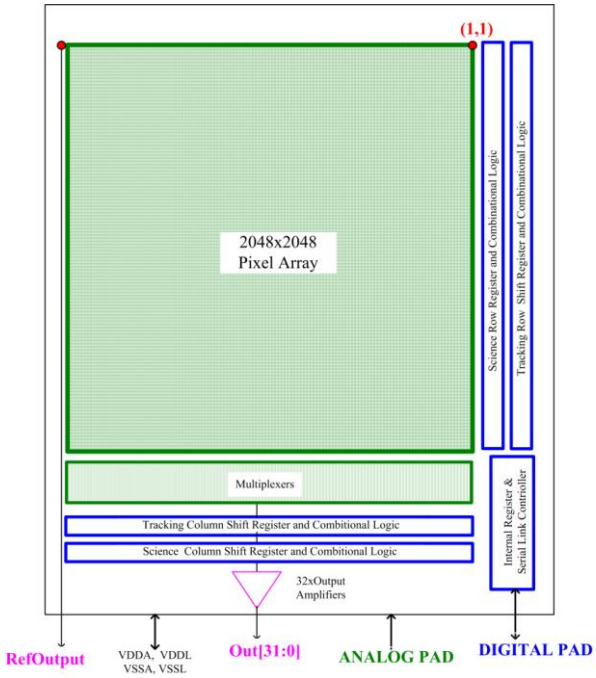

Figure 3: ALFA ROIC Synoptic

3.1.3 Hybridized Prototype Detector design

The Detection Layer is hybridized with the Silicon ROIC by Indium bumps, and a specific underfill is implemented in the area of interconnection between the two subparts for reliability aspects.

The test package consists of two major components:

- a detector package, constituted by:
  - a retina glued on baseplate with a three legs design,
  - a support carrier,
  - a diaphragm mounted above the retina in order to avoid parasitic reflection.
- a flex assembly, constituted by:
  - a standard rigid PCB flex technology: single structure, same ground plane on rigid and flex zone, separation of digital, video and bias signals,
  - an output connector: NanoD 85 pins (69 useful signals, 16 grounds), body of connector connected to electrical ground.

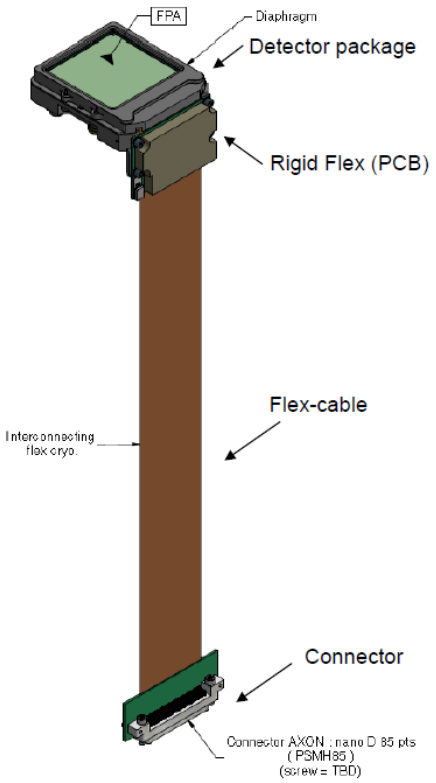

Figure 4: Hybridized Prototype Detector

3.2 Reminder of Detector Manufacturing

3.2.1 Detection Layer Manufacturing

Both the CdZnTe substrate growth and the MCT growth layers followed a routine process that is very well established, and yielded excellent wafers in morphological and crystalline terms.

We originally planned on 3 batches of 2k² detectors and one debugging batch of smaller size, but device fabrication proved trickier than expected. Dedicated and time consuming developments were required by the Hg annealing furnace (compatible with the larger substrate size), the milling of the p-type diode contacts, the etching of metallic levels and in general, achieving uniformity over the larger device area. In the end, we manufactured 3 additional debugging batches and performed a number of short fabrications-characterization loops to resolve all technological issues. Once again, the design of ALFA detectors is identical to that of the CCN4 activity. The overall conclusion for this type of device is positive, in that all issues are now known and solved and the key risks are known. We would expect yields to improve significantly, should we carry on with the activity in the near future.

3.2.2 ROIC and Retina Manufacturing

The ROIC size is approximatively exceeds the limit size of the foundry photo-repetition. Hence, in order to achieve such a large ROIC size, the founder had to develop a stitching technique. This technique has been formerly used in another foundry, but never tested with this one.

After a phase of development, the founder realized a first batch of wafers. This first batch was very important, because it was made to validate stitching and in case this first step succeeded, it should make it possible to test the ROIC at room temperature.

Regarding the first step of validation, it was partially successful. Indeed, the wafers morphology was not perfect about the stitched areas. However, these small defects had no impact on the electrical functionality of the ROIC, thus ROIC testing was possible with these wafers. In the second batch of wafers, the defects were corrected by adjusting the stitching process. The results were very satisfactory, this batch allowed validating definitely the ROIC foundry quality.

When the wafers are received from the foundry, they need a pre-treatment in order to be later used for testing and hybridization. After a first visual inspection, the wafers follow an UBM patterning.

The next step consists in a standard UBM coating aiming to protect the wafer during the ROIC probe test. Actually, the indium bump technology is developed to be coated on the full wafer. The process upscaling to large size wafers was realized in the frame of ALFA development, in order to improve the production capacity at Lynred.

The CMOS ROIC wafers are thinned and glued to a germanium substrate.

The individual ROIC dicing operation is finally realized. Then, each device is analysed through an inspection of indium bump defaults, cracks, chipping, particles, etc...

After the wafers have been post-processed, they are ready to be hybridized.

The first step consists in combining detection circuits and ROIC by pairs. This is actually a critical step due to the very big size of the components. They shall be well matched in shape so that they be associated for hybridization without too much risks to let areas with a bad connection (crushed bumps can lead to cracks or short circuits for instance).

After this combination, the surface of the components is totally cleaned in order to avoid letting in particles which could be trapped after hybridization, leading to a contamination of the component.

Then the Lynred standard hybridization process is applied. This process has been proven on many products in production, however a specific test phase has been led on 2K² components in order to validate its capacity on this type of devices, especially due to its large size.

The underfilling process consists in filling the whole area between the Indium bumps with a specific glue, giving the component an increased reliability. This step has been particularly complicated because the standard glue spreading is not well adapted to such component size. The process had to be adapted in order to obtained satisfying results.

The last operation consists in the antireflective coating layer on the MCT detection layer.

3.2.3 Prototype Detector Manufacturing

The detector manufacturing is made of different steps:

- Retina gluing and positioning: the glue for retina on the baseplate had to be chosen in accordance with previous Lynred studies and heritages.
- Mounting the flex on the support:

  - the support is equipped with two fastening brackets. The screws are thread locked with Loctite 222. Also two indexation screws are implemented for the indexation of the cold shield purpose (white parts)
  - the flex assembly is fixed to the support using 6 screws. The screws are thread locked with Loctite 222.
- Assembly the retina and the support: this operation consists in the assembly of the retina on the supporting device equipped with the flex part. Three clamp nuts with locking device (Loctite 222) are used. The relevant tightening torque is applied.
- Gold wire bonding: the gold wire bonding operation is directly achieved with the support represented here before. A bond pull test is performed before and after on a dedicated mock up. After, an electrical test is achieved. Lynred uses a gold wire wedge bonding process to connect the ROIC to the flex pads.
- Cold shield positioning: the cold shield is screwed on the support by means of four screws. The positioning is assumed by two centering pins previously inserted in the support part.
- Storage tooling and expedition tooling: the same designed tool serves two functions for the detector package:
  - put the detector assembly under clean and safe environment (Dry nitrogen under 1.2 bar)
  - ability to travel in safe conditions (limited possible injuries).

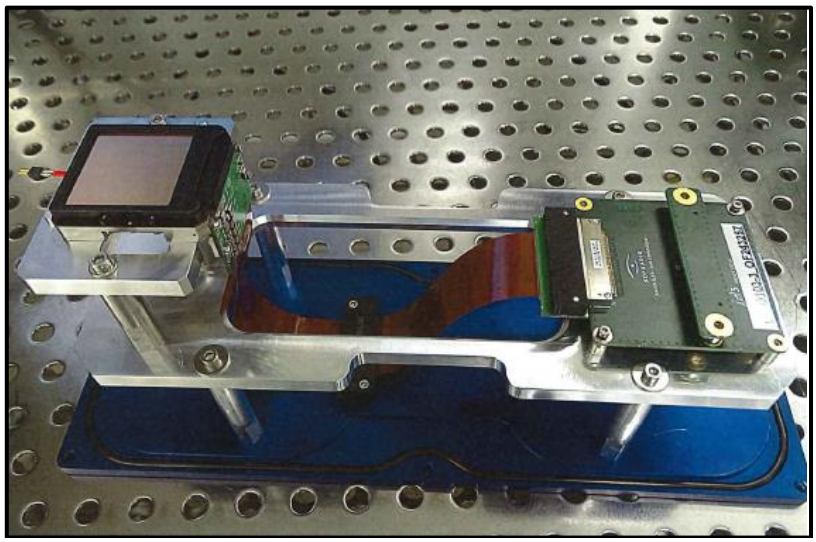

Figure 5 Detector mounted in the tooling

4 REMINDER OF TEST MEANS DESIGN AND VALIDATION

4.1 REMINDER OF TEST MEANS DESIGN

Three test means have been designed for the characterization of the ALFA detectors:

- Verticalix, a cryostat designed mainly for dark current measurements, as well as some measurements under illumination, such as linearity, full well, persistence. The cryostat has been extensively used in previous characterization activities and simply upgraded to host the ALFA devices (Figure 6).
- Quantix, a cryostat designed for quantum efficiency measurements. This test means was specifically developed for the characterization of the ALFA devices, but can also be used in the thermal infrared.
- Intrapix, a test bench designed for the measurement of the intra-pixel response. This test means was specifically developed for the characterization of the ALFA devices, but can also be used in the thermal infrared.

In addition, three more test means are necessary:

- a drive electronic and acquisition system. We purchased the NGC system from ESO, a system identical to the systems that equip all ESO telescopes and drive all their detectors. This allowed a fast and easy implementation of all the necessary configuration files and clocking patterns, as the NGC system already drives the many Teledyne H2RG detectors in the suite of ESO instruments.
- a cryogenic amplifier, which designed is derived from the design of the cryogenic amplifiers developed at ESO for the Teledyne H2RG detectors.
- a calibrated photodiode, for the absolute measurement of incident photon flux and the derivation of the quantum efficiency. This reference detector was built and calibrated at CEA/LETI.

The reason of having two different cryostats is that the measurement of the spectral quantum efficiency requires a monochromator and therefore an entrance window in the cryostat to accept the light from the monochromator. This may lead to too large a cryostat background for the dark current measurements. The Verticalix cryostat has no entrance window and its background is extremely low, making possible the measurement of dark currents as low as a few milli-electrons per second per pixel.

The internal illumination system of the Verticalix cryostat is basic: a small cryogenic black body and a light beam defined by two diaphragms. For this reason, the illumination of the large ALFA devices is not very uniform. The Quantix cryostat has a much more complex cryogenic optical system which delivers a collimated beam, ensuring a very uniform illumination across the ALFA devices, with a goal of 1% non-uniformity of illumination (Figure 7).

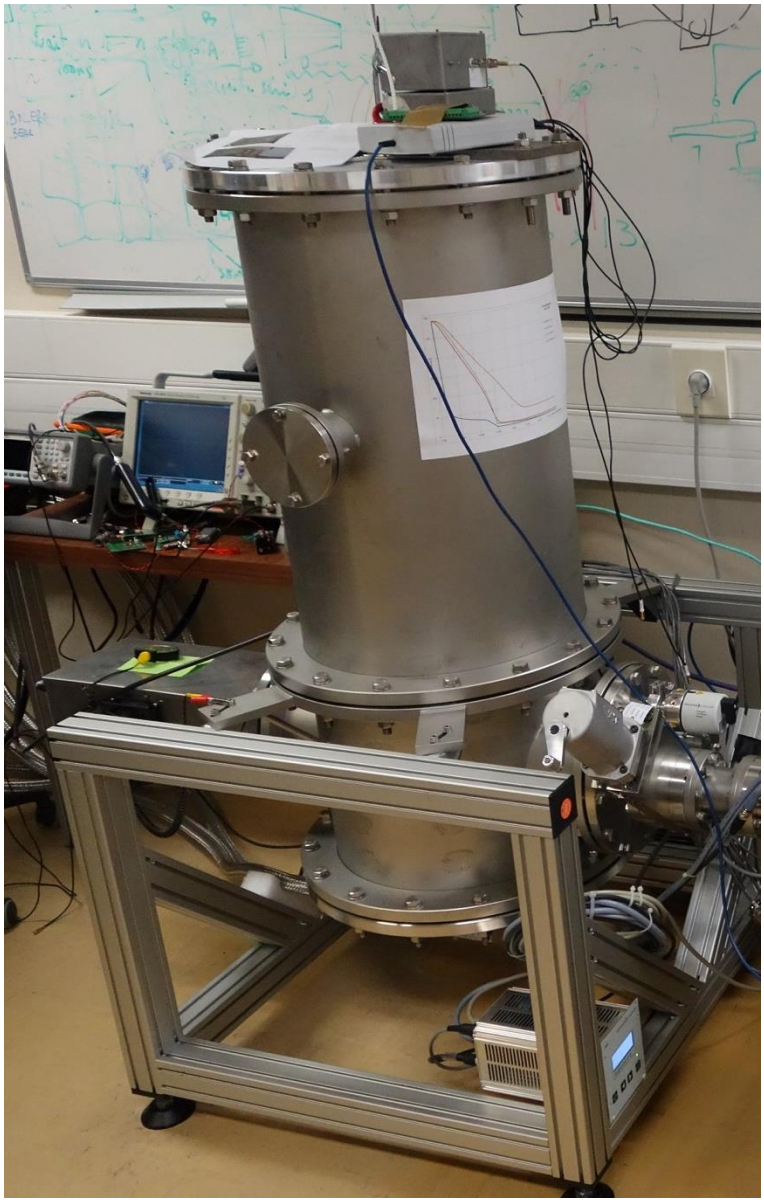

Figure 6 View of the Verticalix cryostat

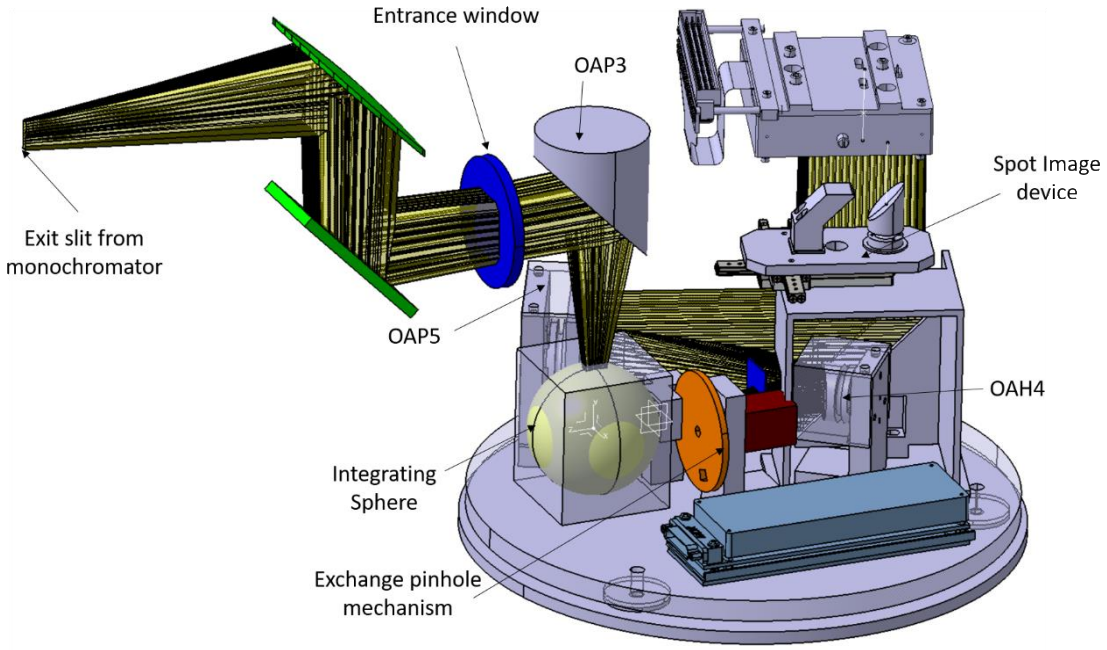

Figure 7 Optical design of the Quantix cryostat. The detector in the top right part of the drawing is a mid-infrared device

The Intrapix bench is based on the use of a continuously self-imaging grating (CSIG) to generate interferences on the detector that excite a number of spatial frequencies. Scanning the CSIG in front of the detector by steps of a fraction of pixel pitch unfold the spatial frequencies. This allows the derivation of the modulation transfer function of the detector, and from there the profile of the intra-pixel response.

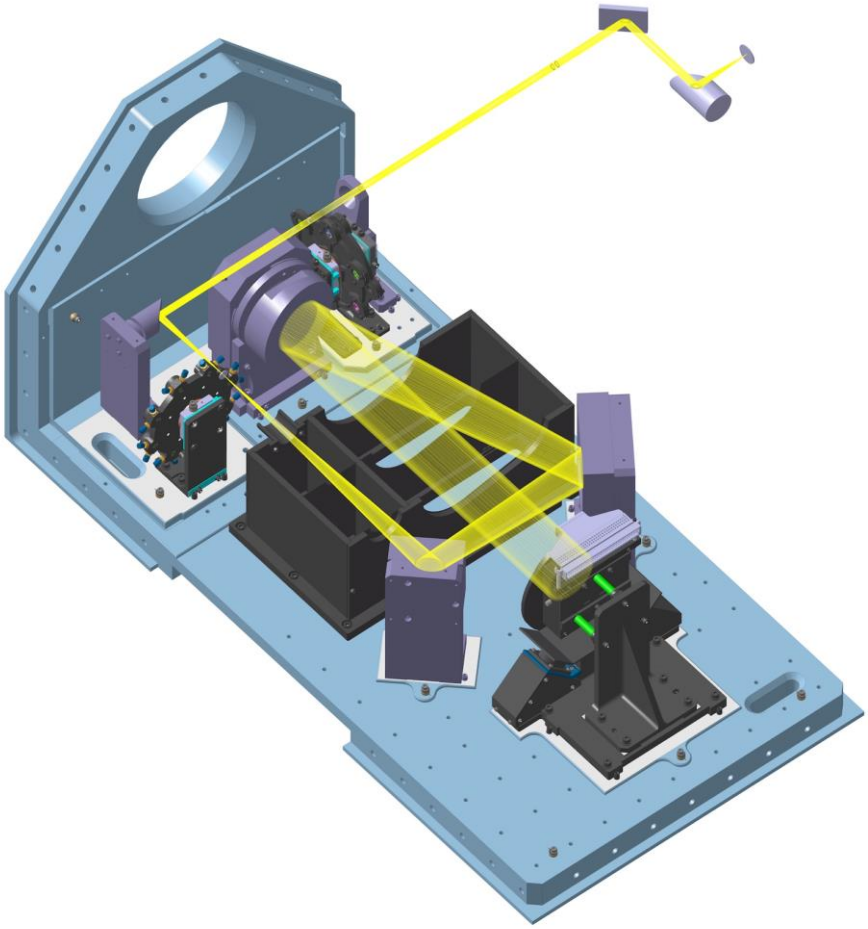

Figure 8 Optical design of the Intrapix bench.

4.2 REMINDER OF TEST MEANS VALIDATION

The Verticalix cryostat was upgraded to accommodate one ALFA detector and its cryogenic amplifier (Figure 9).

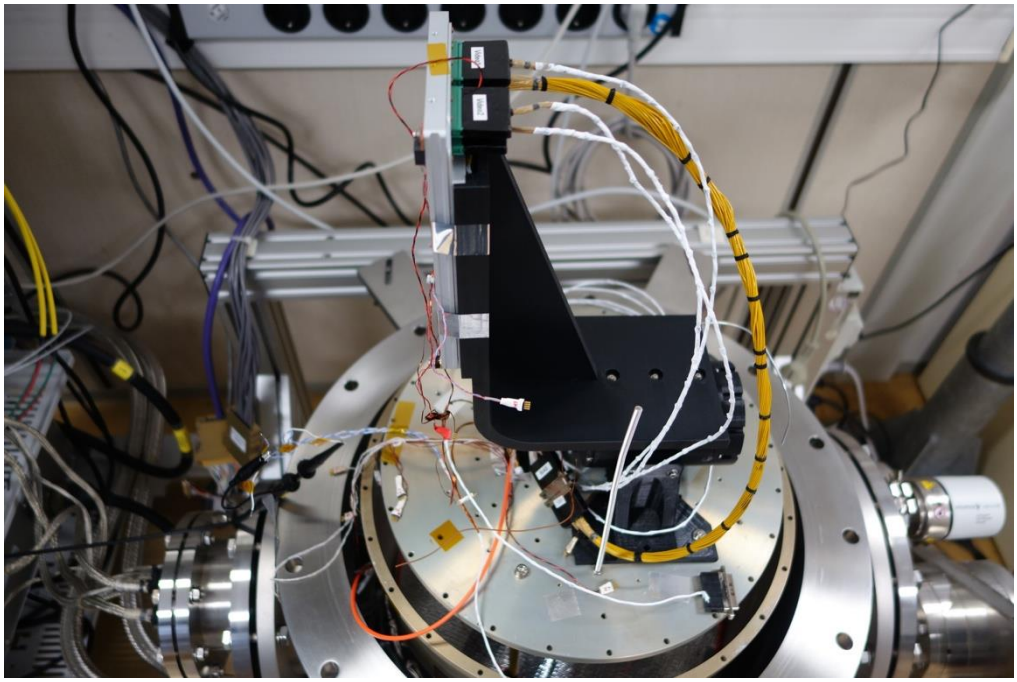

Figure 9 The cryogenic amplifier (grey box) on its mechanical support (in black) in the cryostat. The detector mount is beneath the pre-amplifier mount

Figure 10 shows the Quantix cryostat, and Figure 11 the full Quantix test bench.

Figure 10 The Quantix cryostat

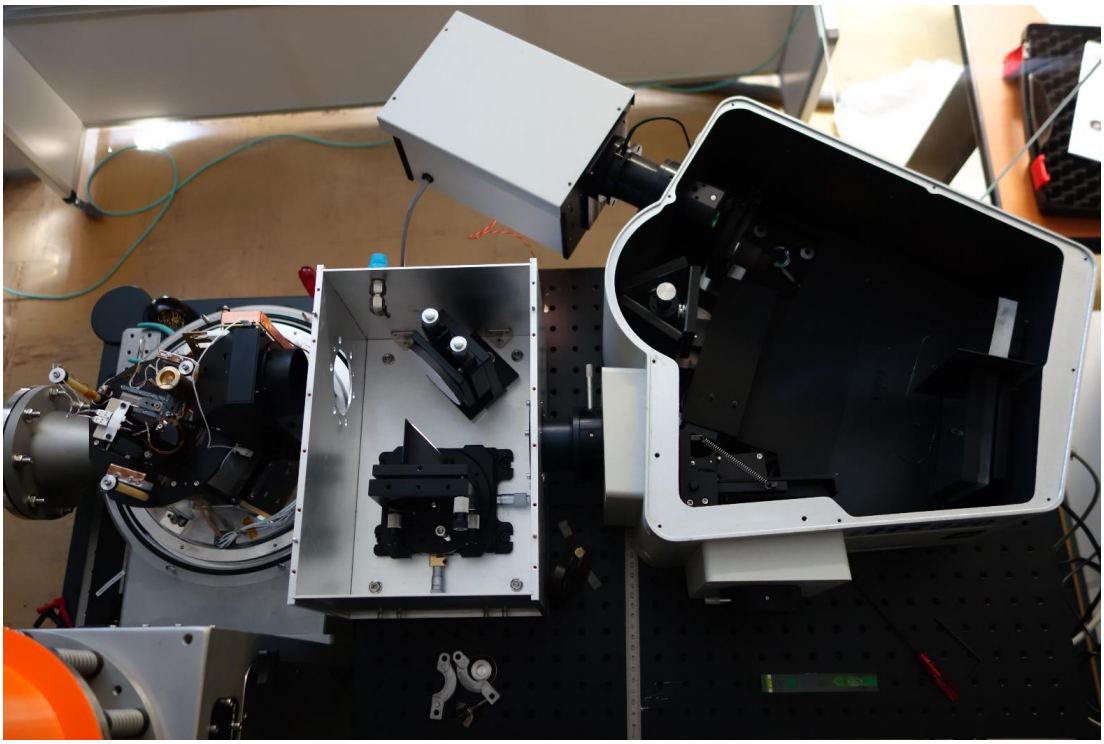

Figure 11 View of the full Quantix test bench, from left to right: cryostat, fore-optics, monochromator

Figure 12 shows the illumination delivered by the Quantix optical system.

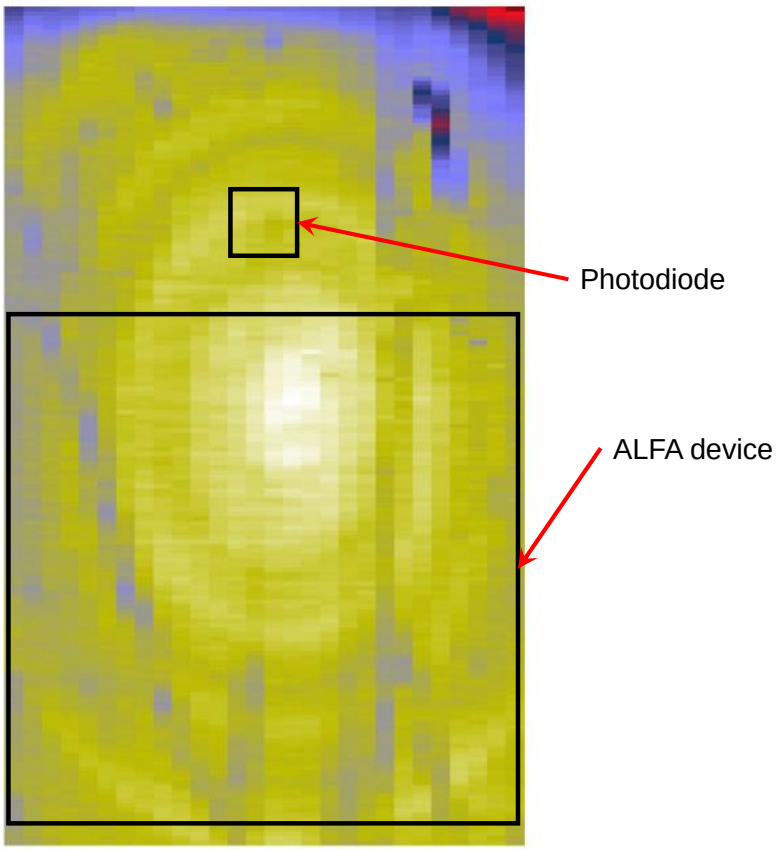

Figure 12 Field of view delivered by the Quantix optical system. The upper part of the field of view is slightly vignetted, but the non uniformity of illumination over the entire field of view is only 2%. The "rings" in the image are the signature of the diamond machining of the mirrors.

The calibrated photodiode (Figure 13) is an avalanche photodiode, with a gain that depends on the bias of the diode (Figure 14). In practice, the bias was set at -3V, giving a gain of 1.54.

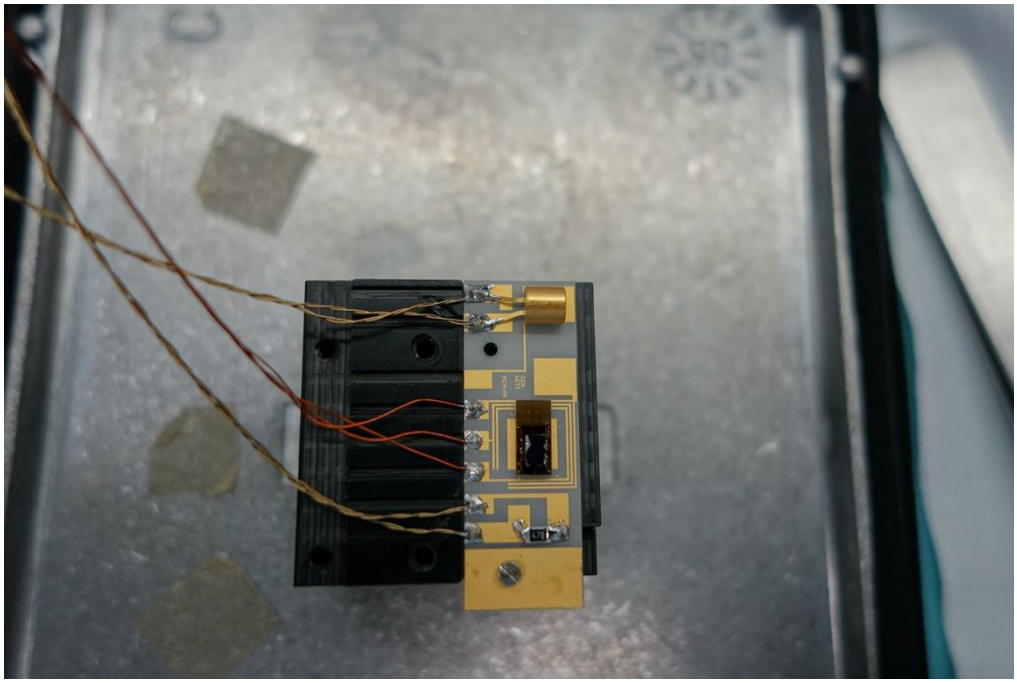

Figure 13 The calibrated photodiode, developed at CEA/LETI

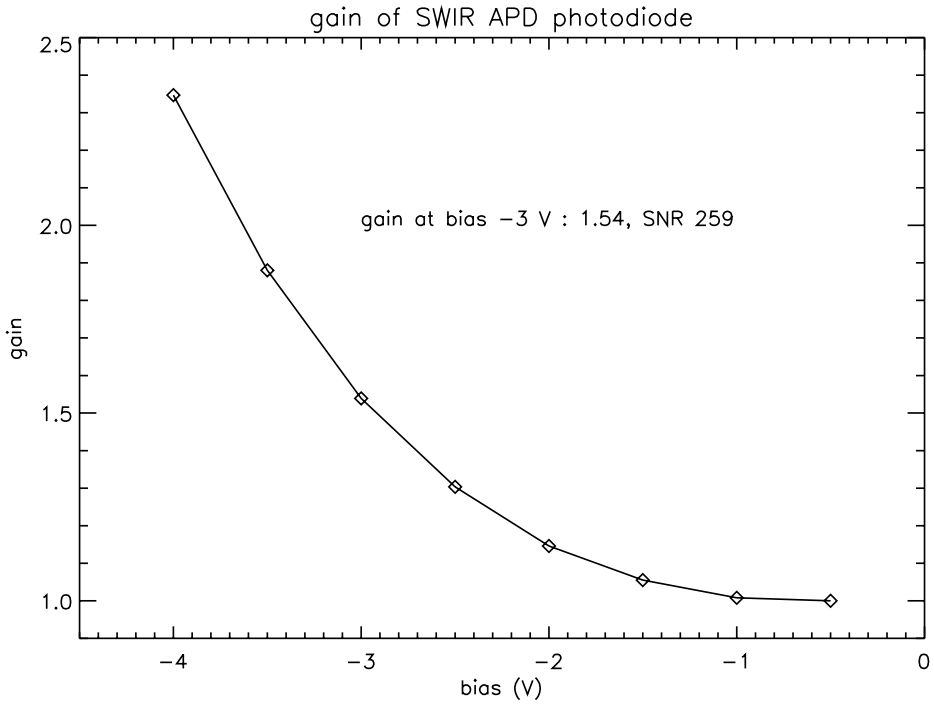

Figure 14 Gain of the photodiode as a function of its bias voltage

The Quantix bench was validated using a detector built at CEA/LETI, characterized at CEA/IRFU, and delivered to ESA in the frame of a previous activity. The quantum efficiency (QE) of this device was measured at ESA/ESTEC. Then the detector was loaned to CEA/IRFU and its quantum efficiency remeasured in the Quantix bench. Figure 15 compares the QE of this device measured at ESA and in Quantix. Both measurements are in very good agreement. The relative uncertainty of both measurements are the same at ±11%, and in both cases, the main contributor to this uncertainty is the calibration of the reference detector.

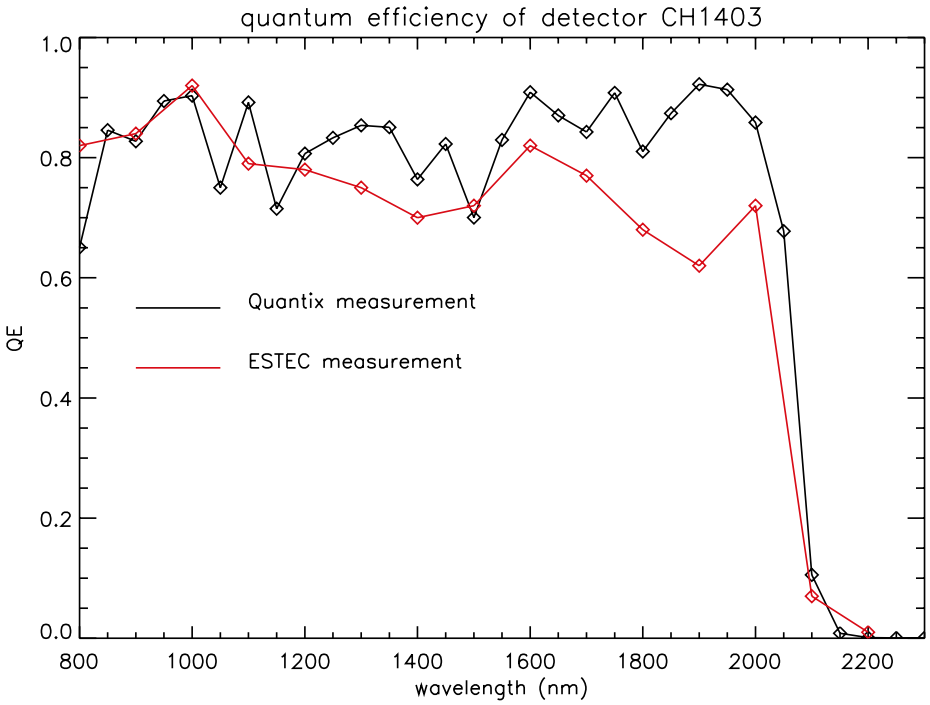

Figure 15 Comparison of ESA and CEA QE measurements for device CH1403

The validation of the Intrapix bench is still ongoing, after a number of technical problems during the manufacturing and testing of the different subsystems (optical bench, cryogenic translation stages). For this reason, the measurement of the intra-pixel response will be performed after the final presentation of the ALFA activity.

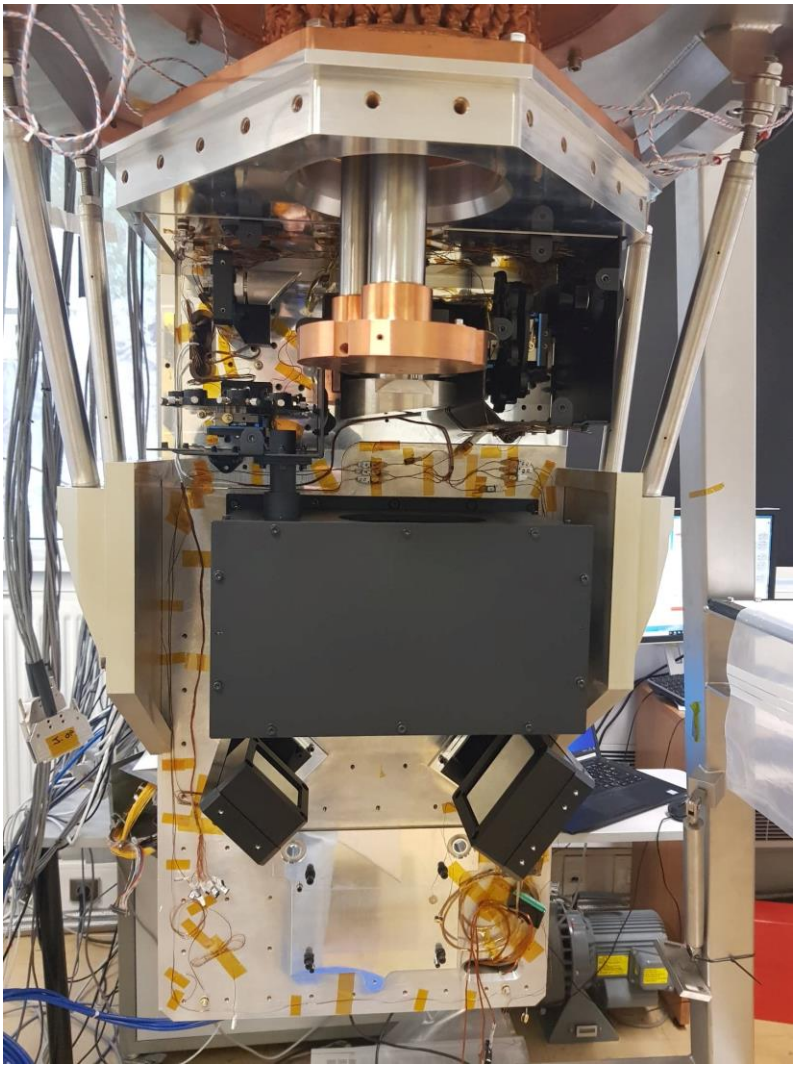

Figure 16 The Intrapix optical bench being integrated in the cryostat

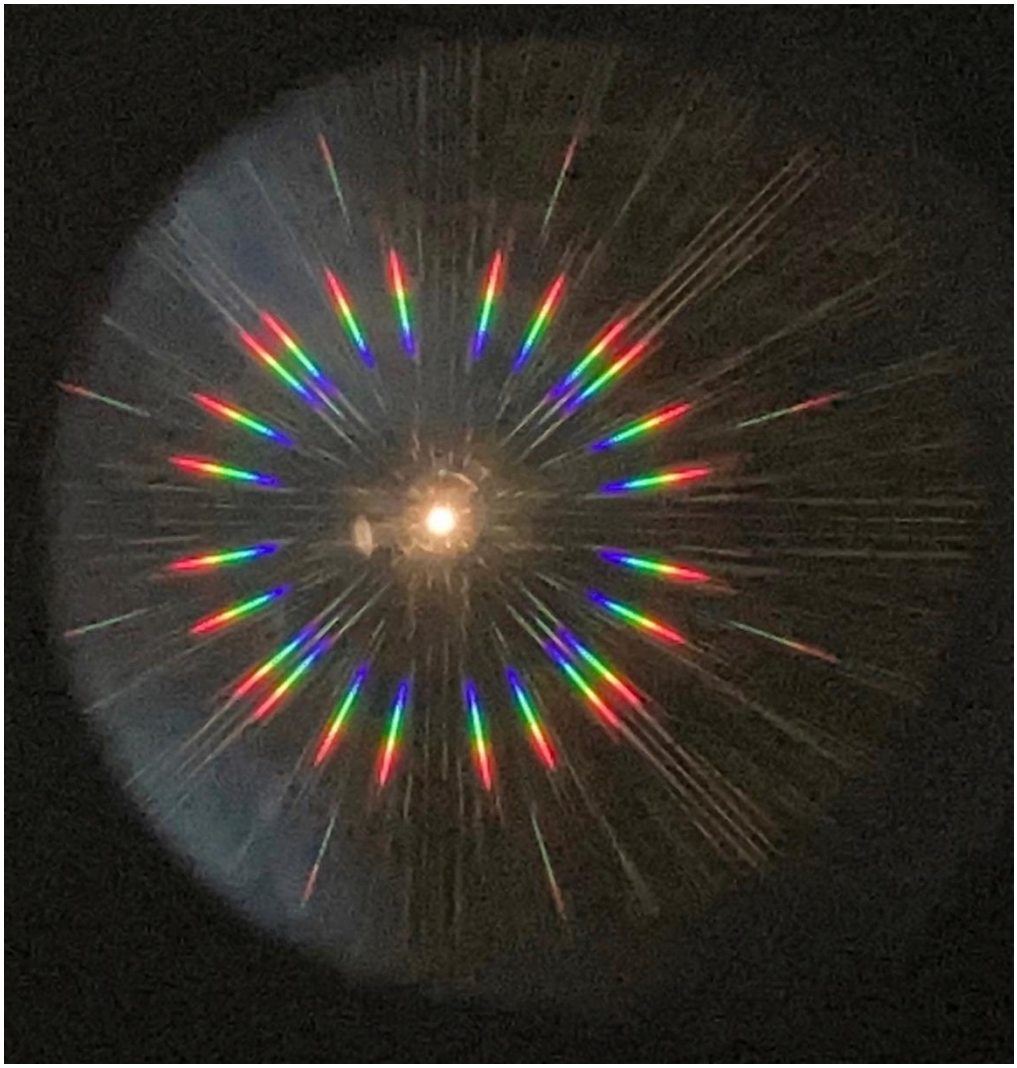

Figure 17 Illumination generated by the CSIG, taken during the alignment of the optical elements of the Intrapix bench

5 DETECTOR PERFORMANCE ANALYSIS & POSSIBLE IMPROVEMENTS

5.1 REMINDER OF DETECTOR PERFORMANCES

5.1.1 ROIC Performances

For the testing at ambient temperature, this step enabled to:

- prove that stitching assembly and foundry process was successful with a good yield considering the huge dimensions of the circuit,
- demonstrate functionality of the circuit (at the exception of some points recalled below, but which do not prevent to operate the circuit in almost all the numerous operating mode),
- give a feedback to ROIC designers to update the datasheet.

The defects detected on the ROIC during the ambient temperature probe test were:

- circuitry to control mode of reset of the pixel (pixel by pixel, line by line, or global) should be fixed to enable to select global mode reset: fixing is accessible in design and fab (by Metal fix),

- reference pixel readout through REFOUT should be fixed such as to be able to readout output voltage from the beginning of the analog transfer function and not only the output source follower: fixing is accessible in design and fab (by Metal fix),
- sensitive pixels under reset should be modified such as to really readout level of pixel under reset as pixels VRST_BR: fixing is accessible in design and fab (by Metal fix),
- in 1 output and 4 outputs science mode: workaround on BIASCOL need to be reported
- test pixel VSUBPD_BR should be modified to prevent short-circuit between VREF and SUBPV: fixing is accessible in design and fab (by Metal fix),
- circuitry should be added to prevent power consumption within output source follower not used in 1 and 4 outputs mode when using internal current sources: fixing possibility to be evaluated if necessary.

Operating the ROIC at cryogenic temperatures was straightforward, the only difference from room temperature being the tuning of the current sources of the two stages of followers. A number of additional defects were found at cold, such as operation of the reference pixels, the row reset, the reference output, … The main issue is the excess readout noise.

5.1.2 Detector Performances

4 ALFA detectors were fabricated and tested at CEA/IRFU, in three batches. 2 of them (1 from batch 1, 1 from batch 2) are functional but with performances out of specifications: one has a very strong short circuit between the two voltages used to bias the diodes, resulting in non-physical performances, one has less than 10% of useable pixels.

The other two devices (1 from batch 1, 1 from batch 3) are functional, with good to very good electro-optical performances. The good device issued from batch 1 shows a very strong cross talk originating in one corner, which impacts the performances over at least half of the device. A number of improvements have been made in the fabrication of the ALFA PV layers between batch 1 and batch 3, with the batch 3 device very clean and very uniform, leading to very good performances.

Still, two major performances are out of specifications: the readout noise and the quantum efficiency.

The excess readout noise was measured in all four hybrid devices, as well as in the bare ROIC. This leads to a readout noise in CDS mode three times larger than the specification.

The QE of both good devices is slightly below specification, around 60-65%. It is still not understood why the QE is lower than the requirement.

The following figures show, for both good devices, the cross talk map, the response map under illumination, the evolution with temperature of the dark current, and the quantum efficiency at 100 K.

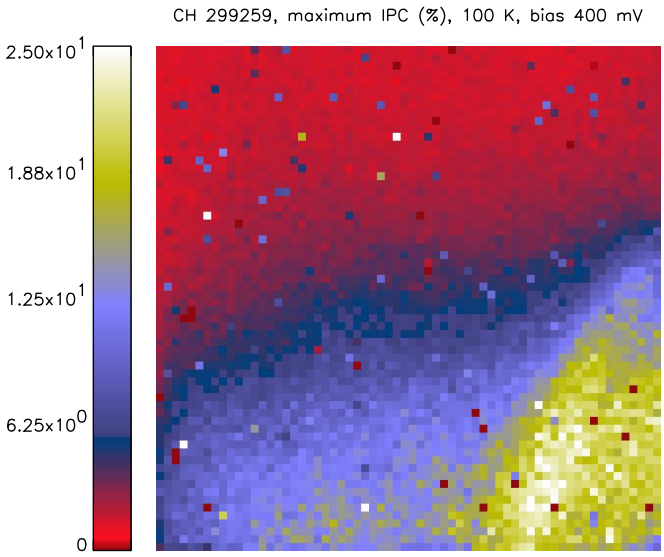

Figure 18 Device CH299259, cross talk map

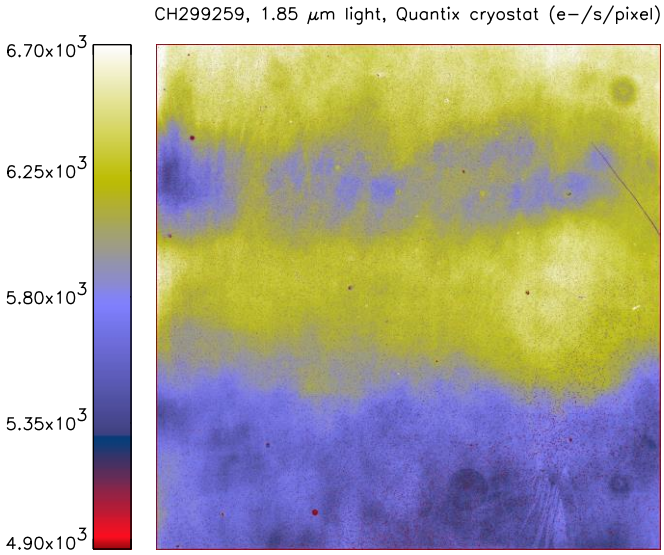

Figure 19 Device CH299259, response map at 1.85 µm

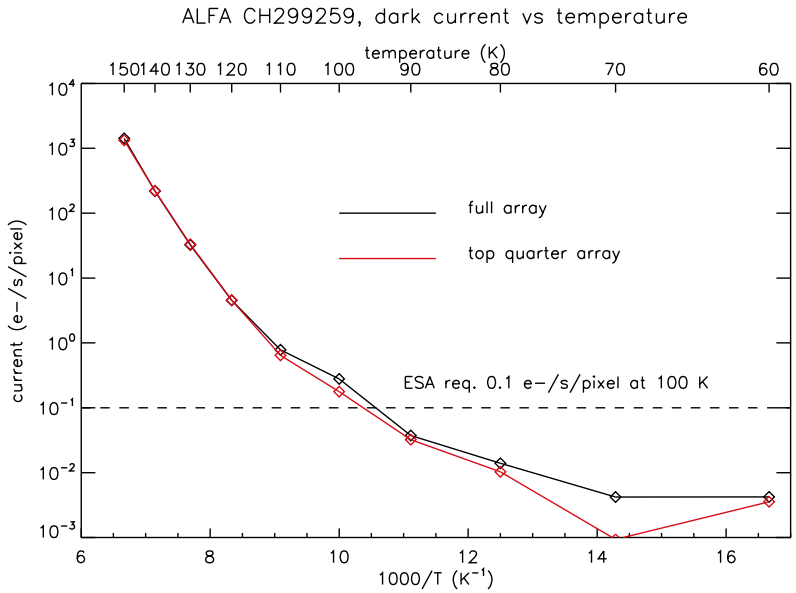

Figure 20 Device CH299259, dark current vs temperature

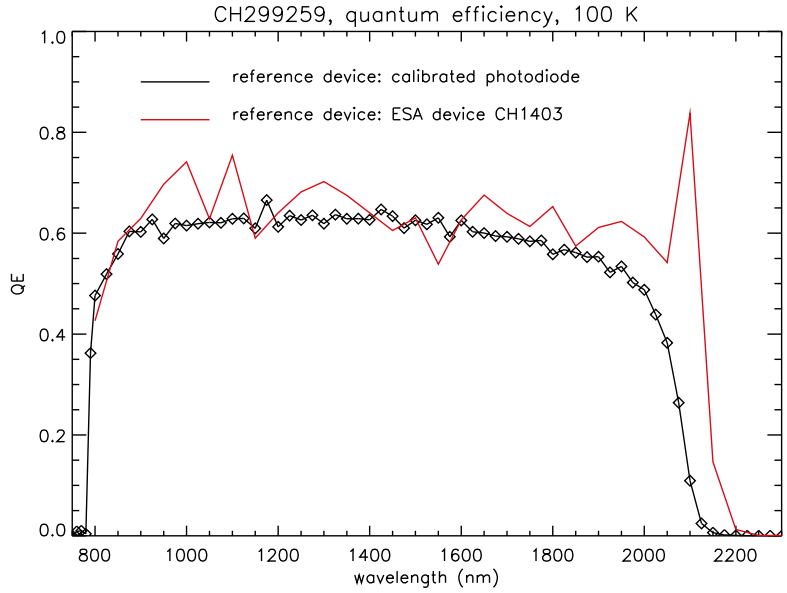

Figure 21 Device CH299259, quantum efficiency at 100 K

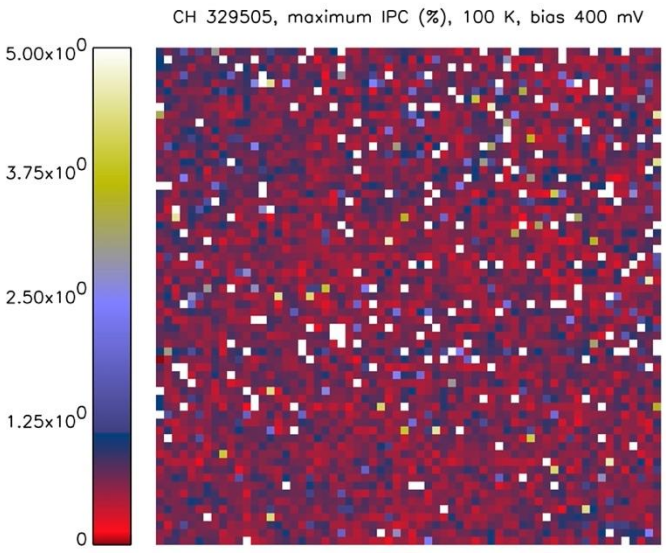

Figure 22 Device CH329505, cross talk map

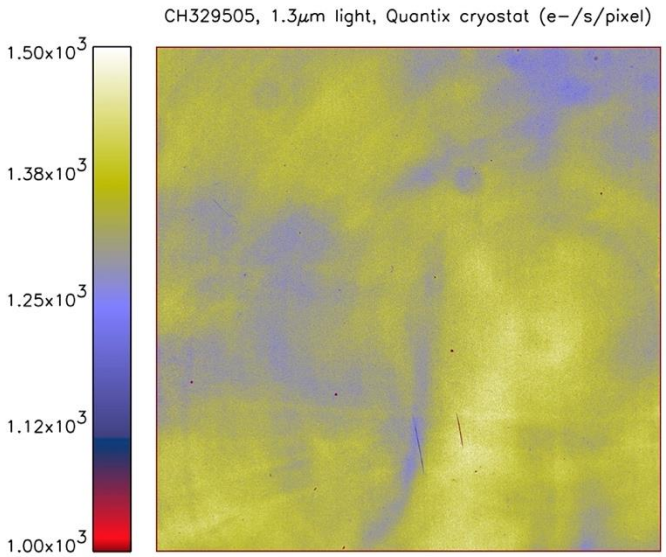

Figure 23 Device CH299259, response map at 1.3 µm

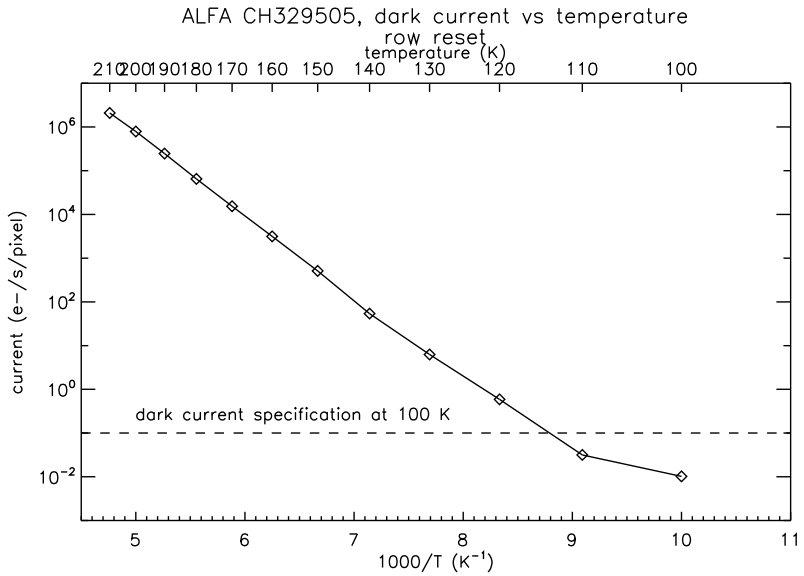

Figure 24 Device CH329505, dark current vs temperature

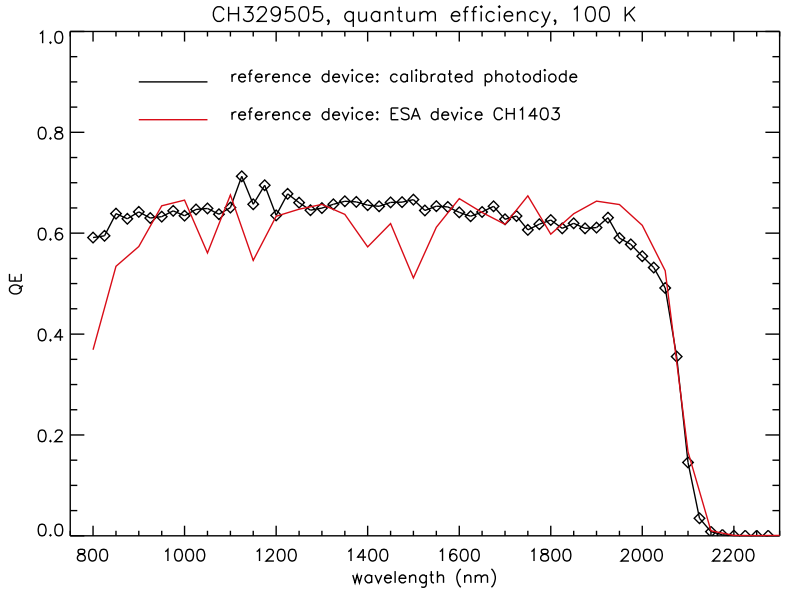

Figure 25 Device CH329505, quantum efficiency at 100 K

5.2 Comparison with Planned Performances and Analysis

The following table compares the performances of the two good devices with the specifications. Note that the measurement of the intrapixel response has not been finished yet, and will be executed only on device CH299259. Device CH329505, from batch 3, is clearly much better than device CH299259 from batch 1, and meets all requirements, with the exception, as explained above, of the readout noise and quantum efficiency.

Requirement No.	Parameter	Value Level 1	CH 299259	CH 329505
PNSA-006	Linear well charge-handling capacity (CHC)	≥ 60 ke-	C: 63 ke-	C: 143 ke-
PNSA-007	Cut-on wavelength	≤ 0.8 µm	C: 0.78 µm	C: < 0.8 µm
PNSA-008	Cut-off wavelength	2.10 +/- 0.05 µm	C: 2.075 µm	C: 2.075 µm
PNSA-009	Quantum efficiency	≥ 70%	NC: 60-65%	NC: 60-65%
PNSA-010	Nominal operating temperature.	100 +/- 1 K	C	C
PNSA-011	Functional temperature range	35 – 300 K	C	C
PNSA-012	Read noise	≤ 18 e-rms	NC: 53 e-	NC: 55 e-
PNSA-013	Total noise	≤ 15 e-rms	NC: 66 e-	NC: 31 e-
PNSA-015	Dark current	≤ 0.1 e-/pix/s	PC: 0.28 e-/pix/s	C: 0.004 e-/pix/s
PNSA-017	Integration time	0 ≤ t ≤ 10000 s	C	C
PNSA-018	PRNU	-	~12%	~6%
PNSA-019	DSNU	-	0.19 e-/pix/s	0.011 e-/pix/s
PNSA-020	Cross-talk (inter-pixel capacitance)	≤ 2%	PC: 1.6%, but large cross talk in bottom right corner	C: 0.8%
PNSA-022	Persistence			
PNSA-023	Non-linearity	< 3%	C: 2.7%	C: 0.3%
PNSA-024	Intra-pixel non-uniformity			
PNSA-032	Pixel operability	99%	NC: 0%, RN excluded: 64.5%	NC: 0%, RN excluded: 97.2%

C: compliant, PC: partially compliant, NC: not compliant

5.3 CONSIDERATION OF DETECTORS AND TECHNOLOGIES SUITABLE FOR SCIENCE APPLICATIONS

The analysis proposed in this document shows that most of the given specifications have been reached (or almost reached) for at least one of the measured detectors, except for quantum efficiency, readout noise and operability.

Regarding the QE, the measurements show values about 60 to 65%, while it was expected to reach around 80% for the technology implemented on the tested detectors. The difference is not explicated.

Regarding the readout noise, the investigations show that kTC noise is not dominant. However, mainly due to the ROIC operational defects, the root cause of the excess noise could not be identified.

Operability measurements are 0% due to the readout noise. Excluding the readout noise of the operability calculation, the result is close to the specification.

As a general conclusion, we can observe that the performances driven by the Detection Circuit (spectral performances, dark current, persistence) are globally very good for at least the last device manufactured, which shows a significant effort realized by CEA on this technology. This is reinforced by the comparisons made with HxRG devices on these parameters.

The performances obtained at ROIC level (especially the readout noise) are more mitigated. However, it is important to recall that it was a first development with such specificities (ROIC size, SFD input stage, different functionalities, modes and reference pixels), and the main challenge at ROIC level was to get a functional device, allowing to make detector measurements and to have a performance status, objective which was reached through this activity.

5.4 PROPOSAL OF POSSIBLE IMPROVEMENTS IN PERFORMANCES

The main improvements identified are at ROIC level. Indeed, the issues encountered with the ROIC are, for most of them, easily correctable in a new design. Afterwards, testing a ROIC exempted from these issues could permit to investigate more in detail and probably better understand its behaviour, and especially the root cause of the readout noise excess.

Regarding the QE, the results were quite different from what we anticipated. Previous QE measurements on this technology were in better accordance with theory. A specific analysis on the possible root causes of these differences would be worthwhile.

Regarding the HgCdTe, the technology could be improved through a “New Generation” technology. The goal would be to improve the manufacturing process (production yield) and the technology uniformity, aspects which could be hardly achievable with the technology processed for the prototype detectors.

5.5 MATURITY LEVEL AND APPLICABILITY TO FLIGHT MODEL MANUFACTURING

The technological parameters considered in this study can be evaluated at different levels of maturity.

Regarding the ROIC, it was quoted at TRL2 at the beginning of the study, mainly because of its large size which requires to use the stitching technique in foundry, and also because of its SFD input stage, very few implemented in Lynred detectors. Making the design and testing ALFA prototypes at operational temperature allowed to go up to TRL4. In order to target low flux space missions, this detector would require first a specific environmental qualification, especially to be evaluated in a radiative environment. Moreover, a huge process development would be necessary, in order to get a more reliable and repeatable production, which was not the case in this study (prototype phase).

Regarding the Detection Circuit, the maturity level is also quoted at TRL4, for the same reasons: design and test were performed and showed very good results. However, to achieve a TRL6 level of maturity necessary to manufacture flight models detectors, an evolution through a “New Generation” technology would be necessary, for the reasons mentioned previously. Thus a huge development would be necessary for reaching such a level of maturity, however this work would be a little bit facilitated as a similar technology evolution is on-going for MWIR and LWIR technologies.

This technological process adaptation would be preliminary before being ready for a technological transfer from CEA to Lynred, which is necessary for a technological production aiming to produce flight model detectors. This was actually done in the frame of other studies. Afterwards, technology maturity improvement would be also linked to its evaluation in a space environment.

To resume, the product developed in the frame of this study would require to be improved in order to facilitate its manufacturing, and probably adapted in terms of design in order that it could be integrated in instruments aiming to answer space missions.

DOCUMENT HISTORY			
Date	Author(s)	Version	Comments
05/05/2023	A. LAMOURE	1.0	First release
15/11/2023	A. LAMOURE	2.0	Update of the document disclosure properties